Scattering of partially coherent electromagnetic fields by microstructured media

Juhani Huttunen* and Ari T. Friberg[†]

Department of Technical Physics, Helsinki University of Technology, FIN-02150 Espoo, Finland

Jari Turunen[‡]

Department of Physics, University of Joensuu, P.O. Box 111, FIN-80101 Joensuu, Finland

Scattering of a two-dimensional, spatially partially coherent electromagnetic field by a two-dimensionally-modulated microstructured medium is treated exactly by means of the coherent-mode representation of the cross-spectral density tensor and a rigorous diffraction theory for fully coherent fields. An explicit method of solution is provided for an isolated groove or slit in a perfectly conducting substrate. The results demonstrate a significant impact of a reduced degree of spatial coherence on the radiant intensity of the field diffracted by such a microstructure. The validity of results obtained on the basis of Kirchhoff's boundary conditions is also assessed.

PACS number(s): 41.20.−q, 42.25.Fx, 42.25.Kb

I. INTRODUCTION

Diffraction and scattering of electromagnetic waves by structured media with wavelength-scale surface-relief or volume corrugations is a subject of major interest in, at least, the optical, infrared, and radio-frequency bands of the electromagnetic spectrum [1]. Approximate methods such as those based on Kirchhoff's boundary conditions are typically inadequate in the characterization of the interaction of electromagnetic radiation with these microstructured media; accurate results can only be obtained by solving Maxwell's equations exactly, taking fully into account the appropriate electromagnetic boundary conditions at surfaces of discontinuity.

Exact analytical solutions of electromagnetic diffraction problems are rare [2], but numerical methods of solution are well established for a wide variety of periodically corrugated surface-relief and volume structures (gratings) [3] and random rough surfaces [4]. In these rigorous investigations of diffraction by microstructured media the incident electromagnetic field has been assumed spatially fully coherent. This assumption can be justified, e.g., in the microwave region and also in the optical region if a single-mode laser is used to provide spatially nearly coherent radiation. However, most sources of electromagnetic radiation are only partially coherent [5]. Besides nonlaser sources important examples are many high-power and semiconductor lasers in photonics applications.

In this paper we put forward a formulation for the electromagnetic scattering of spatially partially coherent fields by microstructured media. We employ the coherent-mode representation of randomly fluctuating wave fields [6] to reduce the general diffraction and scattering problem into several individual problems with fully coherent fields, which are then solved using efficient computational techniques based on rigorous diffraction theory. The solution in the partially coherent case is obtained as an incoherent superposition of these coherent-mode contributions. In materials interactions the technique deals with single-point functions only, as opposed to the usual two-point correlation functions. We consider the diffraction of the so-called Gaussian-Schell-model (GSM) fields [7] by grooves and slits in a perfectly conducting medium. This model is particularly convenient, because it permits a smooth transition from full spatial coherence to complete incoherence, and because the coherent modes of a GSM field are known analytically [8]. These modes are the Hermite-Gaussian functions characteristic of laser resonators and harmonic oscillators.

II. FUNDAMENTALS

A spatially partially coherent, partially polarized, statistically (wide-sense) stationary electromagnetic field at frequency ω may be characterized by four cross-spectral density tensors [5,9] $\mathscr{E}$, $\mathscr{H}$, $\mathscr{F}$, and $\mathscr{G}$. In view of the coherence theory in the space-frequency domain [6], the field is represented by a frequency-dependent random ensemble and the tensors are defined as

$$\mathscr{E}_{kl}(\mathbf{r}_1,\mathbf{r}_2)=\langle E_k^*(\mathbf{r}_1)E_l(\mathbf{r}_2)\rangle\,, \tag{1}$$

$$\mathscr{H}_{kl}(\mathbf{r}_1,\mathbf{r}_2)=\langle H_k^*(\mathbf{r}_1)H_l(\mathbf{r}_2)\rangle\,, \tag{2}$$

$$\mathscr{F}_{kl}(\mathbf{r}_1,\mathbf{r}_2)=\langle E_k^*(\mathbf{r}_1)H_l(\mathbf{r}_2)\rangle\,, \tag{3}$$

$$\mathscr{G}_{kl}(\mathbf{r}_1,\mathbf{r}_2)=\langle H_k^*(\mathbf{r}_1)E_l(\mathbf{r}_2)\rangle\,, \tag{4}$$

where E_k and H_k represent Cartesian components of the electric and magnetic vectors associated with typical real-

*Fax: +358 0 451 3164.

Electronic address: juhani.huttunen@hut.fi

[†]Fax: +358 0 451 3164

Electronic address: ari.friberg@hut.fi

[‡]Fax: +358 73 151 3290.

Electronic address: turunen@cc.joensuu.fi

izations, k and l may assume values x, y, and z, r_1 and r_2 are two spatial points, the brackets denote ensemble averaging, and we have suppressed the ω-dependence for brevity. The tensor elements in Eqs. (1)–(4) are Hermitian, non-negative definite, correlation functions that are connected by Maxwell's equations [10]. The components of the averaged Poynting vector $\langle S(r) \rangle$ associated with a fluctuating field are given by [9]

$$\langle S_j(r) \rangle = \tfrac{1}{4} \sum_{kl} \epsilon_{jkl} [\mathcal{F}_{kl}(r,r) - \mathcal{G}_{kl}(r,r)] , \tag{5}$$

where $j = x,y,z$, summations extend over all Cartesian indices, and ϵ_{jkl} denotes the Levi-Civita antisymmetric unit tensor. The state of polarization generally varies from point to point.

In this paper we restrict, for simplicity, the discussion to diffraction geometries of the type illustrated in Fig. 1. The diffracting object, which in general may contain variations of electric permittivity ϵ, magnetic permeability μ, and conductivity σ, is confined between the planes $z = 0$ and $z = h$, and the material properties are assumed constant if either $z < 0$ or $z > h$. The half-space $z < 0$, from which radiation is incident, consists of a dielectric medium of refractive index $n_r = (\epsilon_r \mu_r / \epsilon_0 \mu_0)^{1/2}$, where ϵ_0 and μ_0 are the vacuum permittivity and magnetic permeability, respectively. In connection with finite transmission, the half-space $z > h$ is similarly taken to be a dielectric medium of refractive index $n_t = (\epsilon_t \mu_t / \epsilon_0 \mu_0)^{1/2}$. On interacting with the microstructured medium the scattered field in the half-spaces $z < 0$ and $z > h$, sufficiently far from the modulated region, behaves locally as a plane wave. Consequently, the far-zone diffraction and polarization properties in both half-spaces maybe described by a directionally dependent 2×2 coherency matrix [2,5] defined as

$$\mathscr{J}_{kl}(r\hat{s}) = \langle E_k^*(r\hat{s}) E_l(r\hat{s}) \rangle , \tag{6}$$

where $r = r\hat{s}$ ($|\hat{s}| = 1$), and the indices k and l now take on the symbols θ and ϕ, which represent the spherical polar angles specifying the direction of the vector $\hat{s}$. In the rationalized mksa system of units, that we are using, the magnetic field in the far zone is $H(r\hat{s}) = (\epsilon/\mu)^{1/2} \hat{s} \times E(r\hat{s})$, where ϵ and μ refer to the uniform medium in question. The averaged Poynting vector and the degree of polarization [2,5] characterizing the far field then are, respectively,

$$\langle S(r\hat{s}) \rangle = \frac{1}{2} \left[\frac{\epsilon}{\mu} \right]^{1/2} \mathrm{Tr}\{ \mathscr{J}(r\hat{s}) \} \hat{s} , \tag{7}$$

$$P(r\hat{s}) = \left[1 - \frac{4 \, \mathrm{Det}\{ \mathscr{J}(r\hat{s}) \}}{[\mathrm{Tr}\{ \mathscr{J}(r\hat{s}) \}]^2} \right]^{1/2} , \tag{8}$$

where $\mathrm{Tr}\{ \mathscr{J}(r\hat{s}) \}$ and $\mathrm{Det}\{ \mathscr{J}(r\hat{s}) \}$ are the trace and determinant of the coherency matrix $\mathscr{J}(r\hat{s})$.

Further simplifications take place if the material properties are strictly y-invariant in the modulated region $0 < z < h$ and the incident field is assumed two-dimensional and linearly polarized such that the electric vector E (TE polarization) or the magnetic vector H (TM

polarization) of each realization points in the y direction. We know, by symmetry, that scattered fields in these situations will be similarly polarized. In TE polarization, for example, the electric field is fully specified by the component $E_y = E_\phi$ and the only surviving element of the coherence matrix (6) is $\mathscr{J}_{\phi\phi}(r\hat{s}) = \langle |E_y(r\hat{s})|^2 \rangle$. The far-zone Poynting vector (7) then reduces to

$$\langle S(r\hat{s}) \rangle = \frac{1}{2} \left[\frac{\epsilon}{\mu} \right]^{1/2} \langle |E_y(r\hat{s})|^2 \rangle \hat{s} . \tag{9}$$

According to Eq. (8), $P(r\hat{s}) = 1$ as expected, i.e., despite partial coherence the diffracted far field now is fully polarized. Analogous expressions and conclusions hold in TM polarization in terms of the sole magnetic field component $H_y = H_\phi$.

In the analysis of microstructure interactions the field's state of coherence plays an important role. In TE polarization the entire cross-spectral tensor $\mathscr{E}$ has but one nonzero element $\mathscr{E}_{yy}$, namely,

$$\mathscr{E}_{yy}(x_1,z_1,x_2,z_2) = \langle E_y^*(x_1,z_1) E_y(x_2,z_2) \rangle , \tag{10}$$

which characterizes the spectral correlations of the electric vector y-component E_y of the fluctuating electromagnetic field. Maxwell's equation $H(r) = (i\omega\mu)^{-1} \nabla \times E(r)$ implies that, for each realization, the nonvanishing components H_x and H_z of the magnetic field vector H are determined by E_y. Thus, in the case of a linearly TE-polarized field, all nonvanishing elements $\mathscr{H}_{xx}$, $\mathscr{H}_{xz}$, $\mathscr{H}_{zx}$, $\mathscr{H}_{zz}$, $\mathscr{F}_{yx}$, $\mathscr{F}_{yz}$, $\mathscr{G}_{xy}$, and $\mathscr{G}_{zy}$ of the four cross-spectral tensors given by Eqs. (1)–(4) are completely specified once we know $\mathscr{E}_{yy}$. For example, $\mathscr{H}_{xx}(x_1,z_1,x_2,z_2) = (\omega\mu)^{-2} \partial^2 \mathscr{E}_{yy}(x_1,z_1,x_2,z_2)/\partial z_1 \partial z_2$. Similarly, in the case of a linearly TM-polarized field, the knowledge of $\mathscr{H}_{yy}$ defined in analogy with Eq. (10) determines the spatial coherence properties of the entire electromagnetic field.

Following Wolf [6] we consider the (absolutely square-integrable) electric cross-spectral tensor component $\mathscr{E}_{yy}^{(i)}$ associated with the incident field across a plane $z = z_0 = \mathrm{const}$ and, by Mercer's theorem, express it in the form

$$\mathscr{E}_{yy}^{(i)}(x_1,z_0,x_2,z_0) = \sum_{q=0}^{\infty} \lambda_q \phi_q^*(x_1) \phi_q(x_2) , \tag{11}$$

where λ_q are the eigenvalues and $\phi_q(x)$ the orthonormal eigenfunctions of the homogeneous Fredholm integral equation

$$\int_{-\infty}^{\infty} \mathscr{E}_{yy}^{(i)}(x_1,z_0,x_2,z_0) \phi_q(x_1) dx_1 = \lambda_q \phi_q(x_2) . \tag{12}$$

The functions $\phi_q(x)$ represent the spatially fully coherent natural modes of oscillation of the partially coherent field at $z = z_0$, and the coefficients λ_q, which are non-negative and of which at least one is nonzero, correspond to the relative weights of these so-called coherent modes. In view of Eq. (11), the coherent modes ϕ_q are mutually uncorrelated and the corresponding fields thus propagate without interference. In a medium of refractive index n_r the coherent-mode contributions obey the usual Helm-

holtz equation with wave number $n_r k = n_r \omega / c$, where $c = (\epsilon_0 \mu_0)^{-1/2}$ is the vacuum speed of light. The spatial evolution of the mode fields is conveniently accounted for by using the angular-spectrum representation containing, in general, both homogeneous and evanescent plane waves; explicit expressions are given in subsequent sections. Denoting the propagated modes by $\psi_q(x,z)$, we then obtain from Eq. (11)

$$\mathscr{E}_{yy}^{(i)}(x_1,z_1,x_2,z_2) = \sum_{q=0}^{\infty} \lambda_q \psi_q^*(x_1,z_1) \psi_q(x_2,z_2) \ , \qquad (13)$$

where $\psi_q(x,z_0) = \phi_q(x)$. Hence, if we know the coherent modes for the incident field, we may treat each mode and its interaction with the modulated region individually in the solution of the diffraction problem.

Once the scattered fields generated by the coherent modes in the regions $z \leq 0$ and $z \geq h$ are solved, as indicated below, the electric cross-spectral tensor elements $\mathscr{E}_{yy}^{(r)}$ and $\mathscr{E}_{yy}^{(t)}$ associated with the partially coherent reflected and transmitted fields are obtained as superpositions similar to Eq. (13). More specifically, if $\chi_q(x,z)$ represents the reflected (in $z \leq 0$ and propagating towards negative z values) or the transmitted (in $z \geq h$) mode contribution produced by $\psi_q(x,z)$, the corresponding electric-field tensor components are

$$\mathscr{E}_{yy}^{(r,t)}(x_1,z_1,x_2,z_2) = \sum_{q=0}^{\infty} \lambda_q \chi_q^*(x_1,z_1) \chi_q(x_2,z_2) \ . \qquad (14)$$

In TM polarization expressions analogous to Eqs. (13) and (14) are obtained quite similarly in terms of the magnetic cross-spectral tensor components $\mathscr{H}_{yy}$. We emphasize that Eqs. (13) and (14) are exact field representations because of the linearity of Maxwell's equations but they are not coherent-mode decompositions in the sense of Eqs. (11) and (12). The number of coherent modes that must be included in the diffraction analysis depends on the state of coherence of the incident field. For a nearly coherent field only a few coherent modes have significant values of λ_q, whereas a large number of modes is typically necessary to represent a globally incoherent field accurately.

Let us now assume that the transmitted mode contribution $\chi_q(x,z)$ is known across some transverse plane, e.g., $z = z' \geq h$. We may express the mode field within the region $z \geq z'$ in the form of an angular spectrum of plane waves as

$$\chi_q(x,z) = \int_{-\infty}^{\infty} T_q(\alpha) \exp\{i[\alpha x + t(\alpha)(z - z')]\} d\alpha \ , \qquad (15)$$

where

$$T_q(\alpha) = \frac{1}{2\pi} \int_{-\infty}^{\infty} \chi_q(x,z') \exp(-i\alpha x) dx \ , \qquad (16)$$

$$t(\alpha) = \begin{cases} [(kn_t)^2 - \alpha^2]^{1/2} & \text{if } |\alpha| \leq kn_t \\ i[\alpha^2 - (kn_t)^2]^{1/2} & \text{otherwise} \ . \end{cases} \qquad (17)$$

Next we introduce polar coordinates (r, θ_t) such that $x = r \sin\theta_t$, $z = r \cos\theta_t$, and let $kr \rightarrow \infty$ along a fixed direction θ_t in the half-space $z \geq h$ (see Fig. 1). Applica-
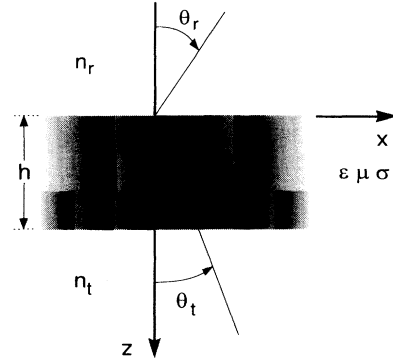
FIG. 1. Geometry for diffraction of a spatially partially coherent electromagnetic field by a structured object, which is confined between the planes $z = 0$ and $z = h$.

tion of the method of stationary phase [11] to the integral in Eq. (15) then yields

$$\chi_q(r, \theta_t) \sim (2\pi k n_t)^{1/2} \exp(-i\pi/4)$$
$$\times \cos\theta_t T_q(kn_t \sin\theta_t) \frac{\exp(ikn_t r)}{\sqrt{r}} \ , \qquad (18)$$

in full agreement with the result obtained through the use of the usual Hankel-type Green function characteristic of two-dimensional wave propagation [12]. Thus the far-zone distribution of $\mathscr{E}_{yy}(r_1, \theta_{t1}, r_2, \theta_{t2})$ in the half-space $z \geq h$ is

$$\mathscr{E}_{yy}^{(t)}(r_1, \theta_{t1}, r_2, \theta_{t2})$$
$$\sim (2\pi k n_t) \cos\theta_{t1} \cos\theta_{t2}$$
$$\times \sum_{q=0}^{\infty} \lambda_q T_q^*(kn_t \sin\theta_{t1}) T_q(kn_t \sin\theta_{t2})$$
$$\times \frac{\exp[-ikn_t(r_1 - r_2)]}{\sqrt{r_1 r_2}} \ . \qquad (19)$$

Considering the reflected mode contributions $\chi_q(x,z)$ and taking into account the fact that these propagate into the negative half-space $z \leq 0$, an expression similar to Eq. (19) is found also for the reflected far-field electric cross-spectral tensor element $\mathscr{E}_{yy}^{(r)}(r_1, \theta_{r1}, r_2, \theta_{r2})$, if angle θ_r now is measured from the negative z axis (see Fig. 1), $T_q(\alpha)$ is replaced by the corresponding reflected angular spectrum $R_q(\alpha)$, and the refractive index n_t of the medium is changed to n_r.

For two-dimensional fields the radiant intensity, which is a measure of the angular distribution of energy flow in the far zone, may be defined as

$$J(\hat{s}) = r|\langle S(r\hat{s}) \rangle| \ , \quad \text{when } r \rightarrow \infty \ . \qquad (20)$$

Using Eqs. (9), (10), (19), and (20) we then obtain for a linearly TE-polarized, spatially partially coherent, transmitted field the expression

$$J(\theta_t) = \left[\frac{\pi}{\omega\mu_t}\right](kn_t)^2$$

$$\times \cos^2\theta_t \sum_{q=0}^{\infty} \lambda_q |T_q(kn_t \sin\theta_t)|^2 . \tag{21}$$

An analogous expression holds for the radiant intensity of the reflected field in terms of μ_r, n_r, θ_r, and R_q. The distinction between TE and TM polarizations shows in the angular spectra T_q and R_q. In addition, the first factor on the right-hand side of Eq. (21) is replaced in TM polarization by $\pi/\omega\epsilon_t$ or $\pi/\omega\epsilon_r$ for the transmitted or reflected field, respectively.

III. DIFFRACTION OF COHERENT FIELDS BY GROOVES AND SLITS

We showed that the general diffraction problem with partially coherent illumination can be reduced, by use of the coherent-mode decomposition, into a set of diffraction problems with coherent fields. In general, the latter can be solved by a variety of mathematical techniques. In complex scattering configurations the calculations may be tedious, utilizing, e.g., finite-element or integral methods, but a considerable advantage is gained in that normally the solution is required only for a limited number of coherent modes.

Below the scattering of partially coherent electromagnetic fields by microstructures is illustrated using the diffraction geometries presented in Fig. 2. With linearly polarized waves and fully conducting media these configurations are simple enough to allow analytic representations of a coherent electromagnetic field within the modulated region. The structures are also of practical
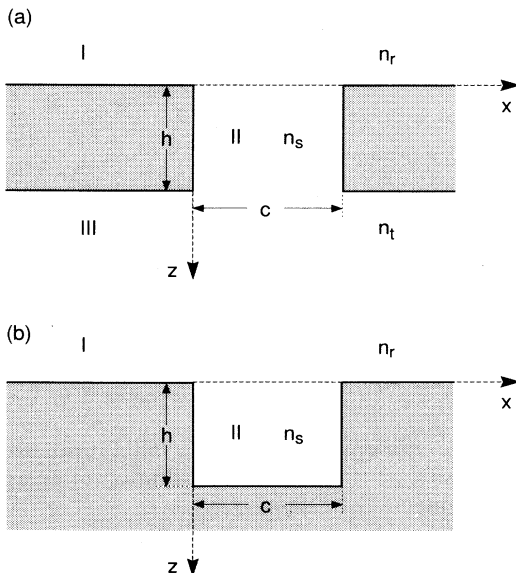
FIG. 2. Geometry for diffraction of a two-dimensional, linearly polarized, electromagnetic field by (a) a slit and (b) a groove in a perfectly conducting screen.

importance because they are encountered in binary optics such as laser disc pickup systems.

For the numerical calculations we formulate an efficient method which makes use of an angular-spectrum representation of the fields in regions I and III, and a waveguide-mode representation of the field in region II. The mode coefficients are obtained from the boundary conditions. We therefore arrive at methods of the general type considered in Ref. [13]. The technique is capable of dealing with incident fields of rather arbitrary form.

A. Diffraction of a TM-polarized wave by a slit

Consider the geometry of Fig. 2(a), which illustrates diffraction of a monochromatic electromagnetic wave by a slit of which c (not to be confused with the speed of light) pierced in a perfectly conducting screen of thickness h. Let us treat first the case of TM polarization, i.e., the sole nonvanishing component of the magnetic field vector is H_y. In space region I ($z \leq 0$) we may write the solution of the Helmholtz equation in the form

$$H_y^{\mathrm{I}}(x,z) = \int_{-\infty}^{\infty} A(\alpha) \exp\{i[\alpha x + r(\alpha)z]\}d\alpha$$
$$+ \int_{-\infty}^{\infty} R(\alpha) \exp\{i[\alpha x - r(\alpha)z]\}d\alpha , \tag{22}$$

where $A(\alpha)$ denotes the known angular spectrum of the incident field, $R(\alpha)$ represents the unknown angular spectrum of the diffracted field in region I, and

$$r(\alpha) = \begin{cases} [(kn_r)^2 - \alpha^2]^{1/2} & \text{if } |\alpha| \leq kn_r \\ i[\alpha^2 - (kn_r)^2]^{1/2} & \text{otherwise .} \end{cases} \tag{23}$$

Similarly, in region III ($z \geq h$),

$$H_y^{\mathrm{III}}(x,z) = \int_{-\infty}^{\infty} T(\alpha) \exp\{i[\alpha x + t(\alpha)(z-h)]\}d\alpha , \tag{24}$$

where $T(\alpha)$ is the unknown angular spectrum of the diffracted field in this region and

$$t(\alpha) = \begin{cases} [(kn_t)^2 - \alpha^2]^{1/2} & \text{if } |\alpha| \leq kn_t \\ i[\alpha^2 - (kn_t)^2]^{1/2} & \text{otherwise .} \end{cases} \tag{25}$$

In region II ($0 \leq z \leq h$) within the slit aperture we use a waveguide-mode expansion

$$H_y^{\mathrm{II}}(x,z) = \sum_{m=0}^{\infty} X_m(x)\{a_m \exp(i\gamma_m z)$$
$$+ b_m \exp[-i\gamma_m(z-h)]\} , \tag{26}$$

where a_m and b_m are unknown modal coefficients. The condition that E_z must vanish at the perfectly conducting slit boundaries $x = 0$ and $x = c$ gives

$$X_m(x) = \begin{cases} c^{-1/2} & \text{if } m = 0 \\ (2/c)^{1/2}\cos(m\pi x/c) & \text{if } m > 0 \end{cases} \tag{27}$$

and

$$\gamma_m = \begin{cases} [(kn_s)^2 - (m\pi/c)^2]^{1/2} & \text{if } m \leq kn_s c/\pi \\ i[(m\pi/c)^2 - (kn_s)^2]^{1/2} & \text{otherwise ,} \end{cases} \tag{28}$$

where n_s is the refractive index in region II and the func-

tions $X_m(x)$ are orthonormal in the interval $0 < x < c$.

We next apply the electromagnetic boundary conditions at $z = 0$ and $z = h$ to solve for the unknown a_m, b_m, $R(\alpha)$, and $T(\alpha)$. Continuity of H_y across $z = 0$ in the interval $0 < x < c$ gives

$$\int_{-\infty}^{\infty} [A(\alpha) + R(\alpha)] \exp(i\alpha x) d\alpha$$
$$= \sum_{m=0}^{\infty} X_m(x)[a_m + b_m \exp(i\gamma_m h)] . \quad (29)$$

If we multiply Eq. (29) by $X_p(x)$, integrate from 0 to c, define

$$I_p(\alpha) = \int_0^c \exp(-i\alpha x) X_p(x) dx , \quad (30)$$

and make use of the orthonormality of the functions $X_m(x)$, we obtain

$$\int_{-\infty}^{\infty} I_p^*(\alpha)[A(\alpha) + R(\alpha)] d\alpha$$
$$= \sum_{m=0}^{\infty} [a_m + b_m \exp(i\gamma_m h)] \delta_{pm} , \quad (31)$$

where δ_{pm} is the Kronecker delta symbol. By a similar procedure, the continuity of H_y across $z = h$ in the interval $0 < x < c$ gives

$$\int_{-\infty}^{\infty} I_p^*(\alpha) T(\alpha) d\alpha = \sum_{m=0}^{\infty} [a_m \exp(i\gamma_m h) + b_m] \delta_{pm} . \quad (32)$$

Let us next make use of the boundary conditions for E_x, which must be continuous across $z = 0$ in the interval $0 < x < c$ and vanish at the perfectly conducting boundaries if either $x < 0$ or $x > c$. This gives

$$n_r^{-2} \int_{-\infty}^{\infty} r(\alpha)[A(\alpha) - R(\alpha)] \exp(i\alpha x) d\alpha$$
$$= n_s^{-2} \sum_{m=0}^{\infty} X_m(x) \gamma_m [a_m - b_m \exp(i\gamma_m h)] , \quad (33)$$

in the interval $0 < x < c$, with the right-hand side equal to zero elsewhere. Multiplication by $\exp(-i\alpha'x)$, integration from $-\infty$ to ∞, use of the Fourier-integral definition of the Dirac delta function and the orthonormality of $X_m(x)$ yields

$$R(\alpha') = A(\alpha') - \frac{1}{2\pi r(\alpha')} \left[\frac{n_r}{n_s} \right]^2$$
$$\times \sum_{m=0}^{\infty} \gamma_m [a_m - b_m \exp(i\gamma_m h)] I_m(\alpha') . \quad (34)$$

A similar procedure at $z = h$ gives

$$T(\alpha') = \frac{1}{2\pi t(\alpha')} \left[\frac{n_t}{n_s} \right]^2 \sum_{m=0}^{\infty} \gamma_m [a_m \exp(i\gamma_m h)$$
$$- b_m] I_m(\alpha') . \quad (35)$$

If we substitute Eq. (34) into Eq. (31), and Eq. (35) into Eq. (32), and define

$$K_{pm} = \frac{1}{2\pi} \left[\frac{n_r}{n_s} \right]^2 \int_{-\infty}^{\infty} r^{-1}(\alpha) I_p^*(\alpha) I_m(\alpha) d\alpha , \quad (36)$$

$$L_{pm} = \frac{1}{2\pi} \left[\frac{n_t}{n_s} \right]^2 \int_{-\infty}^{\infty} t^{-1}(\alpha) I_p^*(\alpha) I_m(\alpha) d\alpha , \quad (37)$$

we obtain a doubly infinite system of linear equations

$$\sum_{m=0}^{\infty} (\delta_{pm} + K_{pm}\gamma_m) a_m + \sum_{m=0}^{\infty} (\delta_{pm} - K_{pm}\gamma_m) \exp(i\gamma_m h) b_m = 2 \int_{-\infty}^{\infty} I_p^*(\alpha) A(\alpha) d\alpha , \quad (38)$$

$$\sum_{m=0}^{\infty} (\delta_{pm} - L_{pm}\gamma_m) \exp(i\gamma_m h) a_m + \sum_{m=0}^{\infty} (\delta_{pm} + L_{pm}\gamma_m) b_m = 0 , \quad (39)$$

which can be solved for α_m and b_m by standard methods if the summations are truncated. Once a_m and b_m are known, the unknown angular spectra of the diffracted fields in regions I and III are obtained from Eqs. (34) and (35).

B. Diffraction of a TE-polarized wave by a slit

If the incident field is TE polarized, i.e., the sole nonvanishing component of the electric field is E_y, we may still use Eqs. (22), (24), and (26) to represent the fields in region I, III, and II, respectively, provided that H_y is replaced by E_y. The modal functions $X_m(x)$ are given, instead of Eq. (27), by

$$X_m(x) = (2/c)^{1/2} \sin(m\pi x/c) , \quad (40)$$

with $m \geq 1$ instead of $m \geq 0$ because the mode with $m = 0$ vanishes identically.

It remains to apply the boundary conditions used to match the fields at $z = 0$ and $z = h$. In place of Eqs. (36) and (37) we now define

$$K_{pm} = \frac{1}{2\pi} \int_{-\infty}^{\infty} r(\alpha) I_p^*(\alpha) I_m(\alpha) d\alpha , \quad (41)$$

$$L_{pm} = \frac{1}{2\pi} \int_{-\infty}^{\infty} t(\alpha) I_p^*(\alpha) I_m(\alpha) d\alpha , \quad (42)$$

with $I_m(\alpha)$ still given by Eq. (30). The final set of liner equations for the modal coefficients a_m and b_m is now, instead of Eqs. (38) and (39),

$$\sum_{m=1}^{\infty} (K_{pm} + \gamma_m \delta_{pm}) a_m + \sum_{m=1}^{\infty} (K_{pm} - \gamma_m \delta_{pm}) \exp(i\gamma_m h) b_m = 2 \int_{-\infty}^{\infty} r(\alpha) I_p^*(\alpha) A(\alpha) d\alpha ,$$ (43)

$$\sum_{m=1}^{\infty} (L_{pm} - \gamma_m \delta_{pm}) \exp(i\gamma_m h) a_m + \sum_{m=1}^{\infty} (L_{pm} + \gamma_m \delta_{pm}) b_m = 0 .$$ (44)

Once a_m and b_m are solved, $R(\alpha)$ and $T(\alpha)$ are obtained from

$$R(\alpha') = \frac{1}{2\pi} \sum_{m=1}^{\infty} [a_m + b_m \exp(i\gamma_m h)] I_m(\alpha') - A(\alpha') ,$$ (45)

$$T(\alpha') = \frac{1}{2\pi} \sum_{m=1}^{\infty} [a_m \exp(i\gamma_m h) + b_m] I_m(\alpha') ,$$ (46)

which replace Eqs. (34) and (35). It is remarkable that Eqs. (45) and (46), as well as Eqs. (34) and (35), remain valid even when the thickness $h = 0$; this corresponds to an alternative solution of the classic Sommerfeld slit problem [12].

C. Diffraction of a TM-polarized wave by a groove

In the geometry of Fig. 2(b) the boundary condition that E_x be zero at the bottom of the groove transforms the field representation in region II, given by Eq. (26) for a slit, into the form

$$H_y^{\mathrm{II}}(x,z) = \sum_{m=0}^{\infty} X_m(x) \{ \exp(i\gamma_m z)$$

$$+ \exp[i\gamma_m(2h - z)] \} a_m .$$ (47)

It remains to apply the boundary conditions at $z = 0$. The continuity of H_y in the interval $0 < x < c$ gives

$$\int_{-\infty}^{\infty} I_p^*(\alpha) [A(\alpha) + R(\alpha)] d\alpha$$

$$= \sum_{m=0}^{\infty} a_m [1 + \exp(i2\gamma_m h)] \delta_{pm}$$ (48)

and the boundary condition for E_x yields

$$R(\alpha') = A(\alpha') - \frac{1}{2\pi r(\alpha')} \left[\frac{n_r}{n_s} \right]^2$$

$$\times \sum_{m=0}^{\infty} \gamma_m [1 - \exp(i2\gamma_m h)] I_m(\alpha') a_m .$$ (49)

If we insert Eq. (49) into Eq. (48), we obtain for a_m a set of linear equations

$$\sum_{m=0}^{\infty} \{ \delta_{pm} [1 + \exp(i2\gamma_m h)] + \gamma_m [1 - \exp(i2\gamma_m h)] K_{pm} \} a_m = 2 \int_{-\infty}^{\infty} I_p^*(\alpha) A(\alpha) d\alpha ,$$ (50)

where K_{pm} is defined in Eq. (36). Once the modal coefficients a_m are determined, the angular spectrum $R(\alpha)$ associated with the diffracted field in region I is obtained from Eq. (49).

D. Diffraction of a TE-polarized wave by a groove

In TE polarization we obtain, in place of Eqs. (49) and (50),

$$R(\alpha') = \frac{1}{2\pi} \sum_{m=1}^{\infty} a_m [1 - \exp(i2\gamma_m h)] I_m(\alpha') - A(\alpha')$$ (51)

and

$$\sum_{m=1}^{\infty} \{ [1 - \exp(i2\gamma_m h)] K_{pm} + \gamma_m [1 + \exp(i2\gamma_m h)] \delta_{pm} \} a_m = 2 \int_{-\infty}^{\infty} r(\alpha) I_p^*(\alpha) A(\alpha) d\alpha ,$$ (52)

with K_{pm} given by Eq. (41). Obviously Eqs. (49) and (51) are trivially correct in the limit as the groove depth $h \to 0$.

E. Numerical considerations

The numerical solution of the diffraction problem of a coherent field by a groove or a slit contains two computationally critical steps.

In the numerical integration of the expressions for K_{pm} and L_{pm} the range of integration should be chosen such that convergence is achieved. These integrations represent computationally the most time-consuming task, although the integrations in Eq. (30) may be carried out analytically. However, the coefficients K_{pm} and L_{pm} are the same for slits and grooves of different depths, and for all coherent modes associated with the illumination wave. The coefficients K_{pm} and L_{pm} vanish analytically if $p + m$ is odd. For even values of $p + m$, integration over homogeneous plane waves, i.e., when $r(\alpha)$ and $t(\alpha)$ are real, provides the real parts of K_{pm} and L_{pm}, whereas the evanescent waves contribute an imaginary part. The integrand tends rapidly to zero for sufficiently large values of $|\alpha|$, but the required integration range depends on the parameters m and p.

Truncation of the summations in the final set of linear equations must be chosen such that the waveguide-mode amplitudes a_m and b_m, and the complex amplitudes $R(\alpha)$ and $T(\alpha)$ converge satisfactorily. In general, the number of waveguide modes that must be retained in the analysis grows when c/λ or h/λ is increased (λ is the wavelength of the radiation).

IV. LINEARLY POLARIZED GAUSSIAN SCHELL-MODEL FIELDS

We consider the class of fields known as Gaussian-Schell-model (GSM) beams [7] incident on the microstructure. Across the plane of its waist, located at $z = z_0$, the electric cross-spectral tensor component $\mathcal{E}_{yy}$ in TE polarization is given by

$$\mathcal{E}_{yy}(x_1, z_0, x_2, z_0) = W_0 \exp[-(x_1^2 + x_2^2)/w^2]$$

$$\times \exp[-(x_1 - s_2)^2/2\sigma_g^2] , \qquad (53)$$

where W_0 is a constant, w represents the $1/e^2$ half-width (spot size) of the electric energy density distribution and σ_g is the rms width of the complex degree of coherence [9]

$$\mu_{yy}(x_1, z_0, x_2, z_0)$$

$$= \mathcal{E}_{yy}(x_1, z_0, x_2, z_0)$$

$$\times [\mathcal{E}_{yy}(x_1, z_0, x_1, z_0) \mathcal{E}_{yy}(x_2, z_0, x_2, z_0)]^{-1/2} \qquad (54)$$

associated with the linearly polarized electric field. The GSM field becomes fully coherent (a Gaussian beam) in the limit $\sigma_g \to \infty$, and approaches complete incoherence as $\sigma_g \to 0$. When σ_g is small, i.e., $\sigma_g \approx \lambda$ or less, $\mathcal{E}_{yy}$ as well as the other nonzero cross-spectral tensor elements consist of significant amounts of evanescent plane waves,

and so the incident beam no longer represents a free field.

The coherent-mode representation, Eq. (11), is known in analytic form for a GSM field [8]. The coherent modes are given by the Hermite-Gaussian functions

$$\phi_q(x) = \frac{1}{\sqrt{2^q q!}} \left[\frac{2}{\pi w^2 \beta} \right]^{1/4} H_q \left[\frac{x\sqrt{2}}{w\sqrt{\beta}} \right] \exp\left[-\frac{x^2}{w^2 \beta} \right] ,$$

$$(55)$$

where we have defined

$$\beta = [1 + (w/\sigma_g)^2]^{-1/2} . \qquad (56)$$

The quantity β satisfies $0 \le \beta \le 1$ and it is a measure of the global degree of coherence. The modal coefficients, given by

$$\lambda_q = W_p \sqrt{2\pi} \frac{w\beta}{1+\beta} \left[\frac{1-\beta}{1+\beta} \right]^q , \qquad (57)$$

decrease monotonically with the mode index and the rate of decrease depends strongly on the coherence conditions of the field. Finally, the angular spectrum of the modal field (55), calculated in accordance with Eqs. (15) and (16), is given by [14]

(a)

(b)
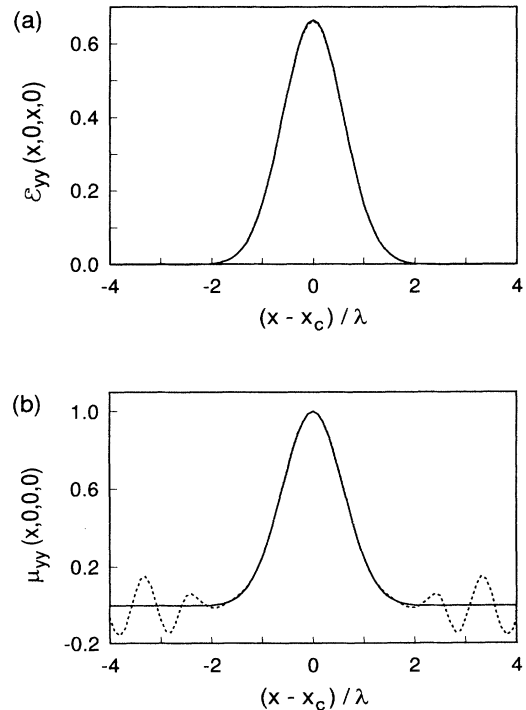
FIG. 3. (a) Distribution of electric energy density $\mathcal{E}_{yy}(x,0,x,0)$ and (b) degree of coherence $\mu_{yy}(x,0,0,0)$ of a GSM field with $w = 1.2\lambda$, $\sigma_g = 0.6\lambda$ (solid curve) and a field with the angular spectrum truncated by an imaging system with $\mathcal{A}_{\text{num}} = 1$ (dotted curve).

$$A_q(\alpha) = \frac{(-i)^q}{2\pi\sqrt{2^q}q!}(2\pi w^2\beta)^{1/4}H_q\left[\frac{1}{\sqrt{2}}w\sqrt{\beta}\alpha\right]$$

$$\times \exp\left[-\frac{1}{4}w^2\beta\alpha^2\right], \tag{58}$$

i.e., it is also a Hermite-Gaussian function. Identical expressions hold in TM polarization for the magnetic cross-spectral tensor element $\mathscr{H}_{yy}(x_1,z_0,x_2,z_0)$.

V. NUMERICAL RESULTS

In the numerical examples we consider a typical situation in microoptics, i.e., a GSM source is imaged onto the plane $z=z_0=0$ by a unit-magnification aberration-free optical system, such that the maximum of the Gaussian distribution of electric energy density coincides with the center, $x=x_c=c/2$, of a groove or a slit. Imaging in other locations and with other magnifications, as well as direct illumination, can be treated without difficulty. In the spirit of Abbe's theory of image formation, we assume that the angular spectrum of each coherent mode is truncated at $|\alpha|=kn_r\sin\theta_{max}=k\mathscr{A}_{num}$, where $\mathscr{A}_{num}$ denotes the numerical aperture of the imaging system. In gen-

eral, the truncation of the angular spectrum modifies $\mathscr{E}_{yy}$ from the Gaussian form of Eq. (53). However, if we assume that $\mathscr{A}_{num}$ is close to unity, such modifications are rather insignificant provided that $w\approx\lambda$ and $\sigma_g\approx\lambda/2$ or larger.

The effects of truncation are illustrated in Fig. 3, where we have plotted the distributions of $\mathscr{E}_{yy}(x,0,x,0)$ and $\mu_{yy}(x,0,0,0)$ assuming that $w=1.2\lambda$, $\sigma_g=0.6\lambda$. Here and throughout the rest of this paper we assume that $n_r=n_s=n_t=1$, take $\mathscr{A}_{num}=1$, and normalize the electric energy density $\mathscr{E}_{yy}(x,0,x,0)$, integrated over the infinite x range, to unity. The distributions of $\mathscr{E}_{yy}(x,0,x,0)$ associated with the original and modified fields are indistinguishable within the plotting accuracy, but the truncation of the angular spectra of the coherent modes $\phi_q(x)$ causes oscillations in the complex degree of spatial coherence $\mu_{yy}(x,0,0,0)$. However, these oscillations are significant only in the region where $\mathscr{E}_{yy}(x,0,x,0)$ is virtually equal to zero. Hence it may be concluded that the parameters w and σ_g associated with the initial field also characterize the truncated field in all examples to be considered.

The influence of a varying degree of spatial coherence in the radiant intensity of a field transmitted by a slit is investigated in Fig. 4. Here we fix $w=4.8\lambda$, $c=2.4\lambda$,
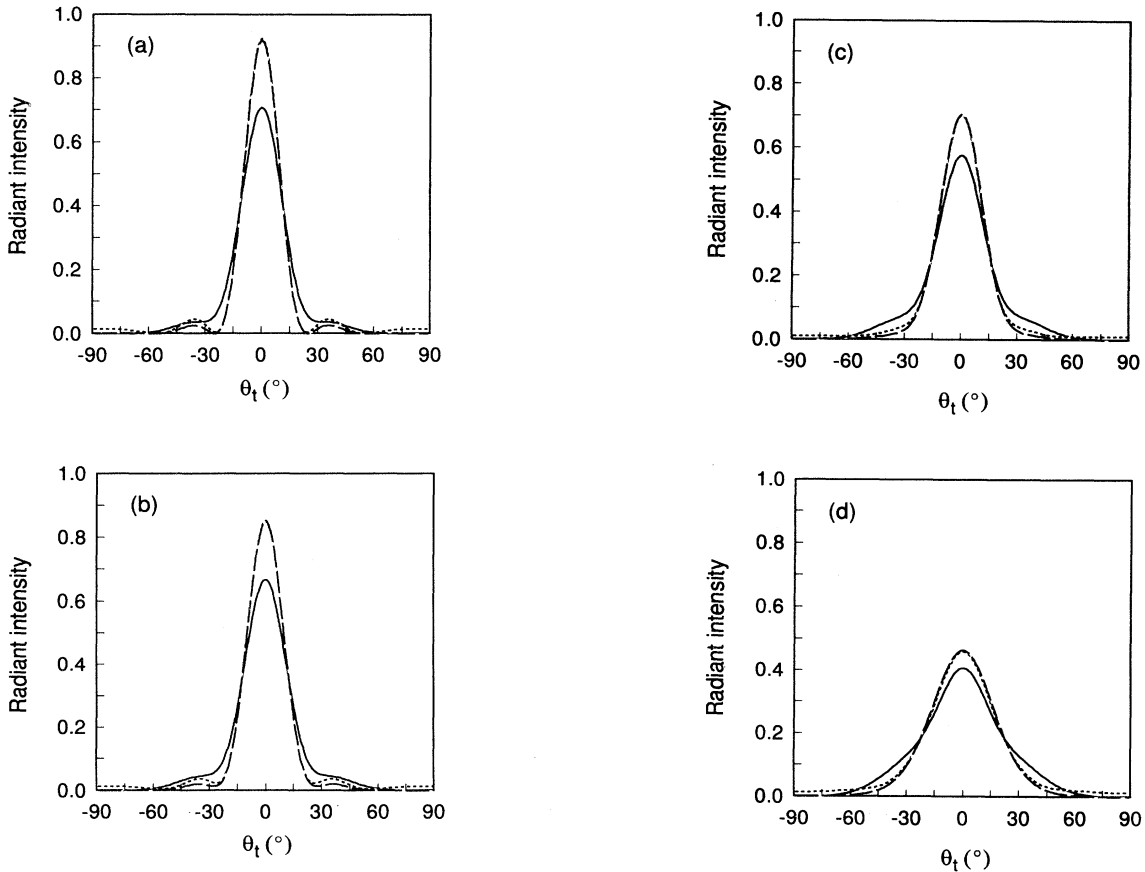
FIG. 4. Radiant intensity of a GSM field with $w=4.8\lambda$ diffracted by a slit of width $c=2.4\lambda$ and depth $h=\lambda$ when (a) $\sigma_g=\infty$, (b) $\sigma_g=2.4\lambda$, (c) $\sigma_g=1.2\lambda$, (d) $\sigma_g=0.6\lambda$. Solid curves: TE polarization. Dotted curves: TM polarization. Dashed curves: approximate results.
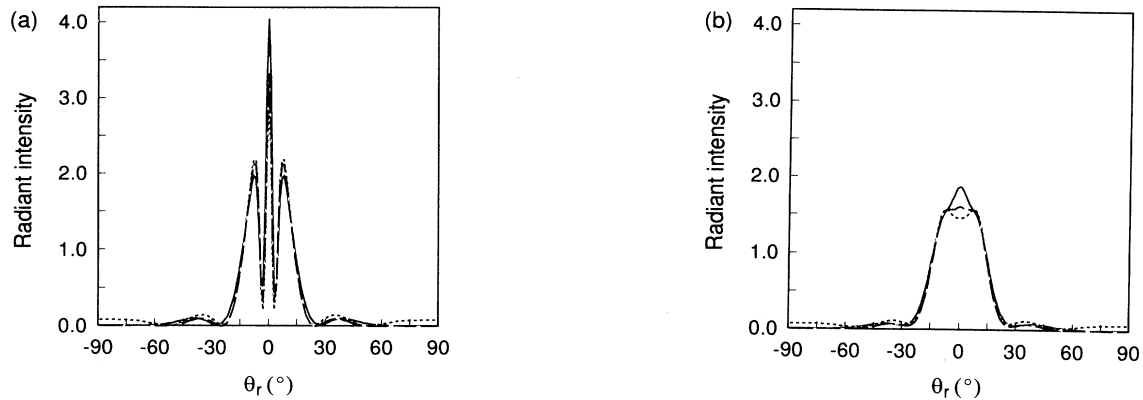
FIG. 5. Radiant intensity of a GSM field with $w = 4.8\lambda$ diffracted by a groove of width $c = 2.4\lambda$ and depth $h = 0.2\lambda$ when (a) $\sigma_g = \infty$, (b) $\sigma_g = 2.4\lambda$. Solid curves: TE polarization. Dotted curves: TM polarization. Dashed curves: approximate results.

$h = \lambda$, and vary σ_g, using a criterion $\lambda_q / \lambda_0 > 10^{-3}$ when choosing the number of coherent modes, Q, retained in the representation of the incident field. This implies that $Q = 1, 9, 15$, and 29, where $\sigma_g = \infty$, 2.4λ, 1.2λ, and 0.6λ, respectively. We display the results for both TE and TM modes of polarization, and compare these to the predic-

tion of an approximate amplitude-transmission mode. In this model we assume, substantially as in Kirchhoff's boundary conditions [2], that the field at $z = h$ is equal, apart from a constant phase factor due to propagation, to the field at $z = 0$ when $0 < x < c$, and the field at $z = h$ vanishes if either $x < 0$ or $x > c$. The model is expected
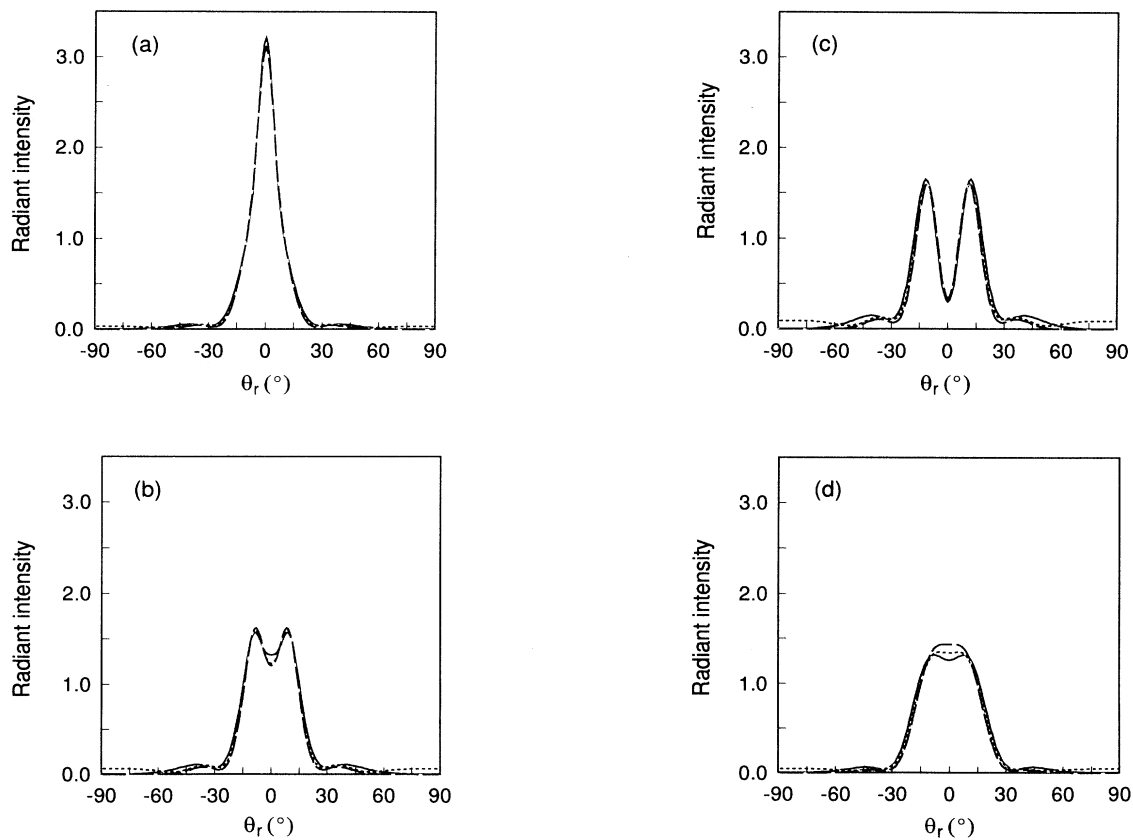
FIG. 6. Diffraction of a GSM field by a groove of width $c = 2.4\lambda$ and depth $h = 0.25\lambda$, when $\sigma_g = 2.4\lambda$ and (a) $w = 9.6\lambda$, (b) $w = 4.8\lambda$, (c) $w = 2.4\lambda$, (d) $w = 1.2\lambda$. Solid curves: TE polarization. Dotted curves: TM polarization. Dashed curves: approximate results.

to be valid when $c \gg \lambda$, at least if the screen thickness h is at most of the same order of magnitude as λ. Rigorous and approximate results for TE polarization are expressed in units of $\pi/\omega\mu$ and for TM polarization in units of $\pi/\omega\epsilon$.

Inspection of Fig. 4(a), which illustrates the case of fully coherent illumination, shows that the results of the approximate model and the rigorous results in TM polarization are nearly identical throughout the paraxial region (diffraction angle $\theta_t \simeq \sin\theta_t$), but the rigorous results in TE polarization differ significantly from these curves. A qualitative explanation of this phenomenon may be found by considering the implications of the electromagnetic boundary conditions at the slit boundaries $x = 0$ and $x = c$, $0 \leq z \leq h$. They require that in TE polarization the dominant field components E_y and H_x vanish at the boundaries but in TM polarization finite values of H_y and E_x are allowed. We recall that the zeroth-order plane-wave mode is permitted in the expansion (26), and departures from the prediction of the approximate model are caused by the excitation of higher-order modes. When $\theta_t \rightarrow \pm\pi/2$, the radiant intensity given by the rigorous method in TM polarization remains nonzero. This is again consistent with the electromagnetic boundary con-

ditions, which permit nonvanishing components H_y and E_z at the boundaries $z = h$ when $x < 0$ or $x > c$.

The general features of diffraction patterns described above persist when the degree of spatial coherence is decreased, as illustrated in Figs. 4(b)–(d). The most visible effect of partial coherence is that the side lobes of the diffraction pattern are smeared, which is in qualitative agreement with previous results in the scalar theory of partial coherence, when the finite slit thickness is neglected [15]. If $\sigma_g \ll c$, we obtain an approximately Gaussian distribution of $J(\theta_t)$, in agreement with the predictions obtained by the quasihomogeneous model of scalar theory of partial coherence [15].

In Fig. 5 we present results similar to those given in Fig. 4, but for a groove of width $c = 2.4\lambda$ and depth $h = 0.2\lambda$, with $w = 4.8\lambda$. We compare the rigorous results to the predictions of an approximate optical-path method, in which we assume that each field realization acquires an additional phase shift of 0.8π radians in the region $0 < x < c$. The optical-path model may be assumed reasonably accurate when $c \gg \lambda$. Clearly, for a groove the polarization effects are less distinctive than they are for a slit in Fig. 4. With coherent illumination the modulation of the radiant intensity is quite pronounced, and its
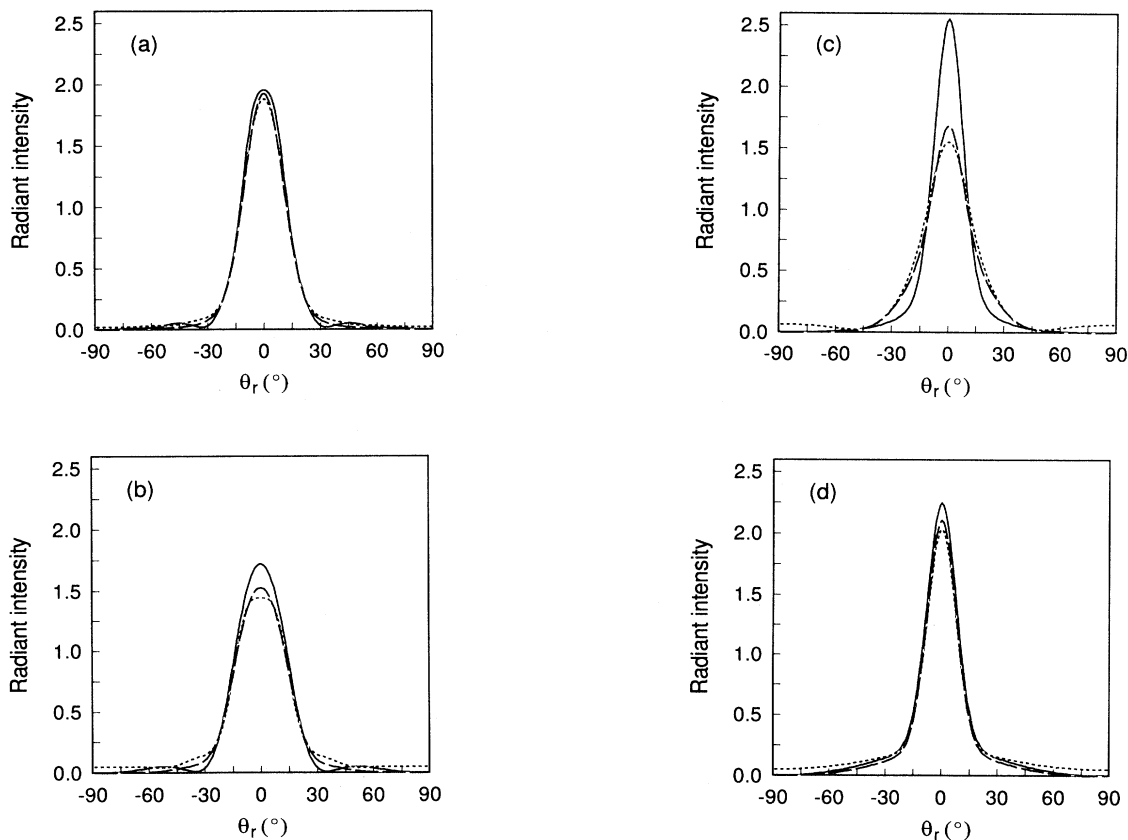
FIG. 7. Diffraction of a GSM field ($w = 4.8\lambda$ and $\sigma_g = 1.2\lambda$) by a groove of depth $h = 1.2\lambda$ and width (a) $c = 4.8\lambda$, (b) $c = 2.4\lambda$, (c) $c = 1.2\lambda$, (d) $c = 0.6\lambda$. Solid curves: TE polarization. Dotted curves: TM polarization. Dashed curves: approximate results.

main features are predicted by the approximate, scalar model. Perhaps more interesting results, which may have technical applications, are obtained when the state of coherence is reduced: Fig. 5(b) indicates the possibility of Gaussian to (nearly) flat-top transformation by diffraction from a simple object. When $\sigma_g < 2.4\lambda$ (not shown), we obtain approximately Gaussian distributions and the polarization effects nearly vanish.

In Fig. 6, we investigate diffraction by a groove with $c = 2.4\lambda$ and $h = 0.25\lambda$ when $\sigma_g = 2.4\lambda$ is fixed, but the width w of the incident field is varied. When $w = 9.6\lambda$, a sharply peaked far-zone pattern is obtained, with perhaps

FIG. 8. Diffraction of a GSM field ($w = 4.8\lambda$ and $\sigma_g = 1.2\lambda$) by a slit of width $c = 1.2\lambda$ and varying depth h with radiant intensity at a polar angle (a) $\theta_t = 0°$, (b) $\theta_t = 15.67°$, (c) $\theta_t = 30°$. Solid curves: TE polarization. Dotted curves: TM polarization. Dashed curves: approximate results.

surprisingly minute differences between the three curves. With $w = 4.8\lambda$ and, in particular, $w = 2.4\lambda$, a doubly peaked pattern results, which can be qualitatively explained in terms of constructive and destructive interference. A nearly flat-top profile is again obtained when $w = 1.2\lambda$, which lends support to our view that smooth beam profile shaping operations can be achieved by optimized wavelength-scale scatterers.

For a groove of fixed depth and an incident field with $w \gg \lambda$, we expect (at least for a coherent field) strongest polarization effects when $c \approx \lambda$. This is indeed verified for a partially coherent field by the analysis given by Fig. 7, where $w = 4.8\lambda$, $\sigma_g = 1.2\lambda$ and $h = 1.2\lambda$ are fixed, and c is varied. With $c = 4.8\lambda$ polarization effects are small, but they increase when $c = 2.4\lambda$ and, in particular, when $c = 1.2\lambda$. These effects reduce again when $c = 0.6\lambda$, which is partly explained by the limited penetration of the field in a groove of subwavelength width irrespective of the state of polarization.

Let us finally examine the effects of the screen thickness h on the far-zone diffraction pattern of a slit with $c = 1.2\lambda$, $w = 4.8\lambda$, and $\sigma_g = 1.2\lambda$. In Fig. 8, we plot the values of $J(\theta_t)$ at $\theta_t = 0°$, $\theta_t = 15.67°$ ($1/e^2$ half-width of the radiant intensity associated with the incident field), and $\theta_t = 30°$. First, it is worth noticing that the perfectly conducting screen modifies the energy distribution compared to the predictions of the approximate model even when $h = 0$. The amplitude transmission results are independent of the screen thickness and, in general, closer to rigorous TM than TE results. Moreover, the TE results stabilize for deep screens far more rapidly than the TM results.

VI. CONCLUSIONS

We have proposed a physically rather general method of solving electromagnetic diffraction and scattering problems with spatially partially coherent illumination. The method makes use of the coherent-mode decomposition of the random field, an angular-spectrum representation of each coherent mode, and a waveguide-mode expansion of the field within the microstructure. In the illustrations a known multimode laser model was used for the incident beam. For other types of illumination different coherent modes apply, and they may be evaluated, for example, computationally. The effects of various relevant parameters, such as the state of coherence and polarization of the incident electromagnetic beam and the dimensions of the scatterer, on the radiant intensity distribution of the scattered field have been analyzed numerically. The exact results were also compared to an optically intuitive scalar model. The present investigation was restricted to simple scatterers, namely, grooves and slits in a perfectly conducting surface, which are of central importance in technologies involving diffractive optics. However, generalizations of the waveguide-mode representation into more complex scatterer configura-

tions, such as those with dielectric and finitely conducting microstructured media, can be realized at the expense of increased computation time. The methodology presented above has rather immediate applications, e.g., to optical micrometrology of lithographically fabricated structures [16].
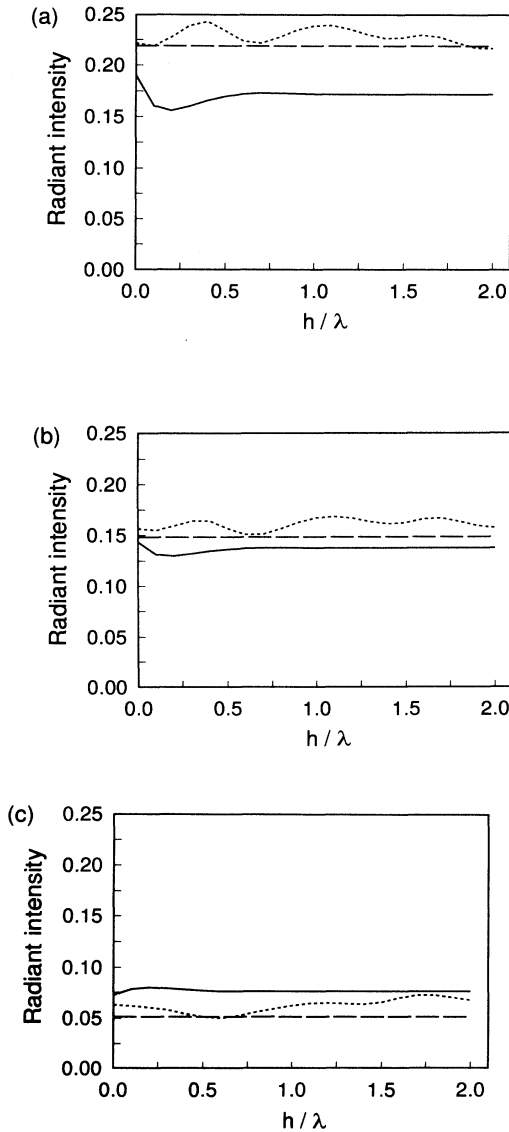
[1] P. Beckmann and A. Spizzichino, *The Scattering of Electromagnetic Waves from Rough Surfaces* (Pergamon, Oxford, 1963).

[2] M. Born and E. Wolf, *Principles of Optics,* 6th ed. (Pergamon, Oxford, 1980).

[3] *Electromagnetic Theory of Gratings,* edited by R. Petit (Springer, Berlin, 1980); T. K. Gaylord and M. G. Moharam, Proc. IEEE **73**, 894 (1985).

[4] See, e.g., the conference special issue: *Modern Analysis of Scattering Phenomena,* edited by J. C. Dainty and D. Maystre, Waves in Random Media **1**, July (1991).

[5] L. Mandel and E. Wolf, Rev. Mod. Phys. **37**, 231 (1965).

[6] E. Wolf, J. Opt. Soc. Am. **72**, 343 (1982); Opt. Lett. **9**, 387 (1984); G. S. Agarwal and E. Wolf, J. Mod. Opt. **40**, 1489 (1993).

[7] A. C. Schell, IEEE Trans. Antennas Propag. **AP-15**, 187 (1967); A. T. Friberg and R. J. Sudol, Opt. Commun. **41**, 383 (1982); R. Simon, E. C. G. Sudarshan, and N. Mukunda, Phys. Rev. A **29**, 3273 (1984).

[8] F. Gori, Opt. Commun. **34**, 301 (1980); A. Starikov and E. Wolf, J. Opt. Soc. Am. **72**, 923 (1982); R. Simon, K. Sundar, and N. Mukunda, J. Opt. Soc. Am. A **10**, 2008 (1993).

[9] J. Perina, *Coherence of Light* (Reidel, Dordrecht, 1985).

[10] C. L. Mehta and E. Wolf, Phys. Rev. **157**, 1188 (1967); E. Wolf, Phys. Rev. D **13**, 869 (1976).

[11] A. Erdelyi, *Asymptotic Expansions* (Dover, New York, 1956).

[12] A. Sommerfeld, *Optics* (Academic, New York, 1954).

[13] O. M. Mendez, M. Cadilhac, and R. Petit, J. Opt. Soc. Am. **73**, 328 (1983); A. Roberts, J. Opt. Soc. Am. A **4**, 1970 (1987); R. A. Depine and D. C. Skigin, *ibid.* **11**, 2844 (1994).

[14] I. S. Gradshteyn and I. M. Ryzhik, *Tables of Integrals, Series, and Products* (Academic, New York, 1965).

[15] E. Wolf, J. Opt. Soc. Am. **68**, 6 (1978); W. H. Carter, Radio Sci. **18**, 149 (1983).

[16] D. Nyyssonen and C. P. Kirk, J. Opt. Soc. Am. A **5**, 1270 (1988).

FIG. 1. Geometry for diffraction of a spatially partially coherent electromagnetic field by a structured object, which is confined between the planes $z = 0$ and $z = h$.